ACS OMEGA

http://pubs.acs.org/journal/acsodf

Article

Molecularly Imprinted Polymeric Sorbent for Targeted Dispersive Solid-Phase Microextraction of Fipronil from Milk Samples

Muhammad Hayat, Suryyia Manzoor,* Nadeem Raza, Akmal Abbas, Muhammad Imran Khan, Noureddine Elboughdiri,* Khalida Naseem, Abdallah Shanableh, Abdullah M. M. Elbadry, Saleh Al Arni, Mhamed Benaissa, and Fatma A. Ibrahim

Cite This: *ACS Omega* 2022, 7, 41437−41448

Read Online

ACCESS | Metrics & More | Article Recommendations | Supporting Information

ABSTRACT: Fipronil, a phenyl pyrazole insecticide, is extensively used in agriculture to control insect infestation. It has the potential to assimilate into the food chain, leading to serious health concerns. We report molecularly imprinted polymer (MIP)-based dispersive solid-phase microextraction for the targeted determination of fipronil in milk samples. Designing such a sorbent is of paramount importance for measuring the accurate amount of fipronil for monitoring its permissible limit. Response surface methodology based on a central composite design following a face-centered approach was used to optimize experimental conditions. The maximum binding capacity of 47 mg g^{-1} was achieved at optimal parameters of time (18 min), temperature (42 °C), pH (7), and analyte concentration (120 mg L^{-1}). Under these conditions, a high percentage recovery of 94.6 ± 1.90% (n = 9) and a low limit of detection (LOD) and limit of quantitation (LOQ) (5.64×10^{-6} and 1.71×10^{-5} μg mL^{-1}, respectively) were obtained. The MIP was well characterized through a scanning electron microscope (SEM) as well as Brunauer−Emmett−Teller (BET), Fourier transform infrared spectroscopy (FTIR), and thermogravimetric analysis (TGA) methods. Adsorption kinetics of the MIP followed the pseudo-first-order model (R^2 0.99 and χ^2 0.96), suggesting the MIP−analyte interaction to be a physiosorptive process, while adsorption isotherms followed the Freundlich model (R^2 0.99). The real sample analysis through high-performance liquid chromatography (HPLC) confirmed the selective determination of fipronil from milk samples.

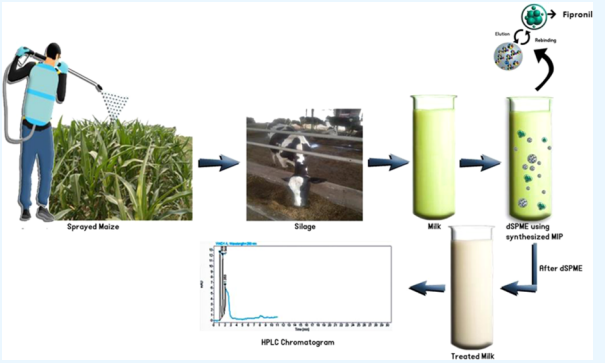

1. INTRODUCTION

The past few decades have undoubtedly witnessed aggravation in pollution on earth. Nowadays, natural water is also being contaminated with myriads of pesticides and insecticides due to their excessive use in agricultural and residential applications. Pesticides may be classified according to their target, mode, and period of action. There are more than 500 different pesticides that are commonly used in our surroundings.[1] Although the use of pesticides has significantly improved the quality as well as quantity of food to cater to the needs of the ever-growing world population, their excessive use has had undesirable effects on nontargeted organisms, including human beings.[2] It is estimated that less than 0.1% of the total pesticides applied to crops reach the targeted pests, while the rest permeate into the environment, contaminating the soil,[3] water,[4] and air.[5]

Fipronil, 5-amino-1-[2,6-dichloro-4-(trifluoromethyl)-phenyl]-4-[(trifluoromethyl)sulfinyl]-1H-pyrazole-3-carbonitrile, phenyl pyrazole, is considered the third most used pesticide in the world market due to its diverse scope and wide range of reactivity.[6,7] By regulating γ-aminobutyric acid (γ-ABA) and causing hindrance in chloride pathways, it interacts with the central nervous system (CNS) of the targeted organism.[8]

Its metabolites, due to their biological activity, may pose risks to nontarget species, including pollinators (bees, bumblebees, moths, and earthworms). Furthermore, these metabolites have also been identified in contaminated soil, water, and plant tissues.[9−11] It has been reported that the half-life of some metabolites of fipronil in the soil is up to 7 months.[12] The residues of fipronil have been detected in different species of plants such as Brassica, Camellia, Ipomoea, and Plantago.[13]

Higher concentrations of fipronil affect agricultural soil greatly by killing beneficial microbial strains and result in lower crop productivity. Consequently, it is pertinent to quantify

Received: August 14, 2022
Accepted: October 24, 2022
Published: November 1, 2022

fipronil even at its trace levels and to abate it in contaminated environments and food samples.

Feeding of animals by sprayed maize having silage creates the possibility of uptake of fipronil in their bodies.[14] In cows, fipronil along with its metabolites can accumulate in adipose tissues and then be excreted through milk and urine.[15,16] Excessive feeding of such silage by feeders could ultimately result in accumulation of residues. Currently, the most popular methods of removing pesticide residues are physical processes, instrumental techniques, and chemical and biological methods.[17] Among these contemporary methods, physical adsorption is considered the most appropriate approach due to its convenience and facile performance.

The direct analysis of fipronil residues from foodstuff using instrumental analytical techniques is difficult due to their complex matrixes and low concentrations.[18]

Molecularly imprinted polymers (MIPs) acquire specific recognition sites that are complementary to the targets in terms of form and functionality. MIPs are promising alternatives to natural and synthetic receptors for analysis in complex matrices due to their premium thermal and chemical stability and selectivity.

MIPs are considered fine separation materials due to their specificity, sensitivity, thermodynamic stability, effective usage in complex samples, template removal and rebounding during extraction, excellent reusability, and low cost. All of these features are attributed to their high demand. Due to their compatibility with other traditional analysis techniques, MIPs have various applications in different fields such as separation science, analytical chemistry, bioenvironmental analysis, and pesticide analysis.[19,20]

Based on the selective properties of imprinted polymers, we selected this technique for the targeted extraction of fipronil from milk samples through dispersive solid-phase microextraction (DSPME).

DSPME is a simple, quick, and economical process for separating, concentrating, and purifying a variety of analytes from real samples with high extraction efficiency, high enrichment factor, and less sample solution consumption. This method, in comparison with SPME, has several advantages, e.g., there is no need of designing a fiber and coating it with a sorbent. Thus, it minimizes the limitations and difficulty of adhering the sorbent on a fiber. It also overcomes the challenges faced due to sorbent swelling in organic solvents. Furthermore, it simplifies the extraction and desorption procedure.[21]

The current study thus describes the designing of a novel MIP for the determination of fipronil in milk samples through DSPME, which has not been reported before. The developed method combines the benefits of specific extraction and the analysis of fipronil as well as miniaturization of the extraction system. The effective optimization of different parameters such as concentration, pH, time, and temperature was evaluated by response surface methodology.

2. MATERIALS AND METHODS

2.1. Chemicals and Reagents. Acrylic acid (AA, purity >99.5%) and acrylonitrile (AN, purity ≥99.5%) were purchased from Merck (Germany). Standard fipronil (99.5%) was obtained from Sigma-Aldrich (Germany) and used as a template. The monomer, vinyl acetate (VA, purity >99%); initiator, benzoyl peroxide (BZO, purity: 99%); crosslinker, ethylene glycol dimethacrylate (EGDMA, purity: 97%); and solvents acetone (purity: 99.5%) and acetonitrile (ACN, purity: 99.8%) were obtained from Fluka USA.

2.2. Synthesis of MIP. Molecularly imprinted polymers for fipronil (template molecule) were synthesized by the coprecipitation method. For the preparation of preassembly solutions, fipronil (0.45 g) was mixed with 20 mL of acetonitrile. After that, 0.3 mL of acrylic acid, 0.25 mL of acrylonitrile, and 0.35 mL of vinyl acetate acting as functional monomers were added, followed by the addition of a crosslinker (3.8 mL of EGDMA) and initiator (0.01 g, BZO). The mixture was sonicated in a water bath for 5 min with continuous nitrogen gas purging. The flask was firmly sealed after nitrogen purging. The solution was heated for 24 h at 70 °C. The resulting polymer was washed with acetone to remove the template molecule and unreacted monomers through Soxhlet extraction. In the absence of a template, the nonimprinted polymer (NIP) was prepared as a blank using the same method as explained above.

2.3. Characterization. A Bruker α II FTIR spectrometer (Bruker, Billerica, MA) equipped with a single reflection diamond automatic refractometer (ATR) module was used to record Fourier infrared spectra for adsorbents in the range of 4000−550 cm^{-1}. A scanning electron microscope (SEM, Hitachi SU8000, Tokyo, Japan) was used to study the surface morphologies of MIP and NIP. Thermogravimetric analysis for the thermal stability of adsorbents was carried out using a TGA unit (Pyris Diamond series, PerkinElmer, Waltham, MA) under a nitrogen atmosphere. MIP and NIP surface area and pore size distribution were measured using a 2000-12, Quanta-chrome Instruments version, 5.1, using the Brunauer−Emmett−Teller (BET) method. The binding capacity was determined using a Shimadzu UV-800ENG240V, SOFT spectrophotometer (Shimadzu, Japan). For chromatographic analysis, an Agilent 1100 liquid chromatograph (Palo Alto, CA) with a quaternary pump, a heated column compartment, a diode array detector (DAD), and an LC workstation was employed.

A 2000-12, Quanta-chrome Instruments version 5.1 was used to achieve Brunauer−Emmett−Teller (BET) and N_2 adsorption−desorption isotherms in the pressure ratio of 0.0658629−0.466542 for analyzing the surface area and pore distribution at 77.3 K. A quantity of 50 mg of dried MIP and NIP was used for analysis. The degassing of all of the samples was carried out under nitrogen flow prior to measurement.

2.4. Response Surface Methodology. Using Design Expert (version 13; Stat-Ease) software, the response surface methodology, which consists of a set of statistical methods for batch optimization and analyzing process factors, was determined. For the model coefficient's determination in quadratic terms, four variables, i.e., pH, time, concentration, and temperature, were used (Table S1). The central composite design (CCD) was built by creating 27 experimental runs to evaluate the binding capacity (Table 2). The binding capacity was calculated with the help of eq 1

$$q_e = \frac{C_0 - C_e}{m} \times V \quad (1)$$

where q_e is the binding capacity, "C_0" and "C_e" are the initial and equilibrium mass concentrations of the analyte in solution, respectively, "V (L)" represents the volume of the solution, and "m (g)" is the mass of the MIP used.

https://doi.org/10.1021/acsomega.2c05217
ACS Omega 2022, 7, 41437−41448

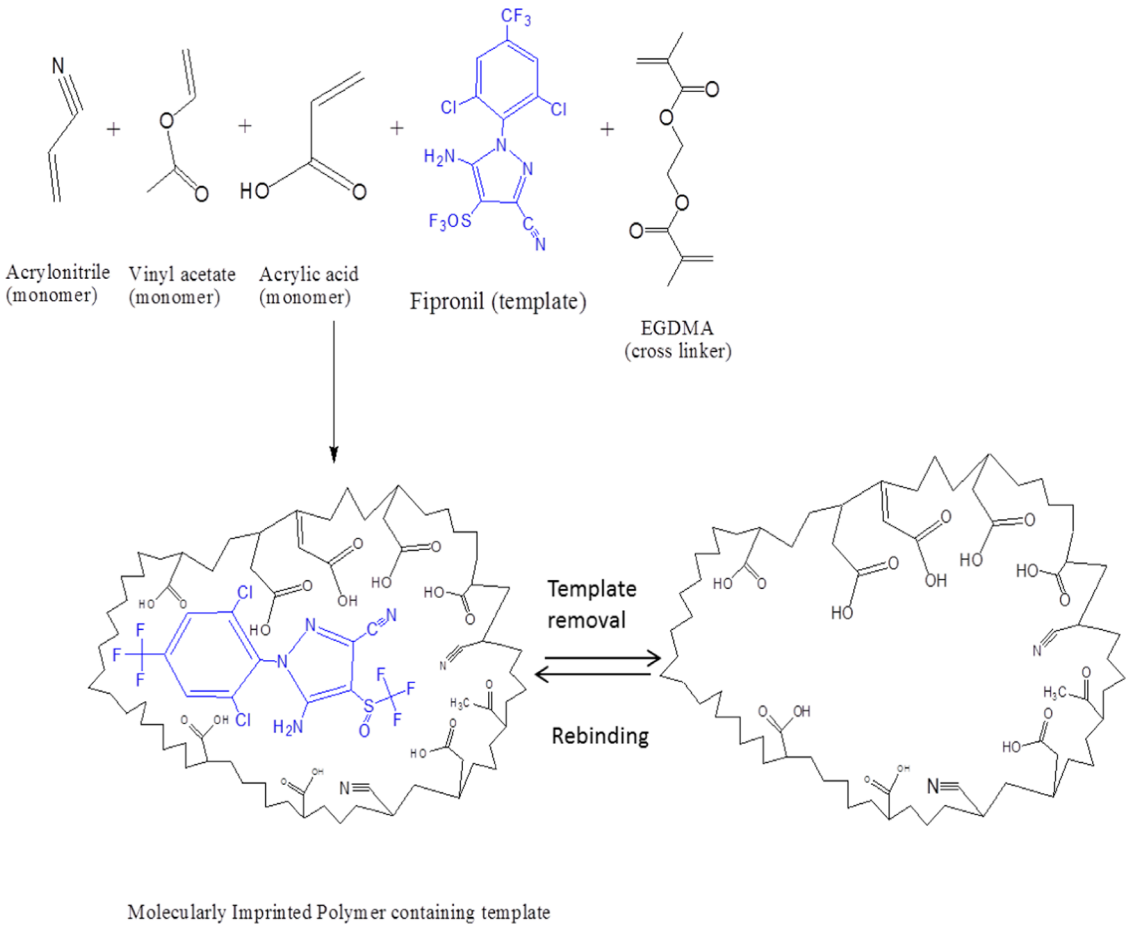

Figure 1. Schematic diagram of the MIP synthesis.

The significance of regression coefficients was evaluated using ANOVA, and RSM experimental sets were designed using Design expert (version 13; Stat-Ease) software.

2.5. Adsorption Isotherms and Kinetic Studies. To apply the adsorption isotherm, a relationship between the binding capacity of MIP and the concentration of fipronil was devised. In a typical experiment, 50 mg of MIP was equilibrated with solutions containing fipronil at various concentrations ranging from 10 to 120 mg L^{-1} for 18 min and filtered using an HPLC-grade filter (0.45 μm). A UV−vis spectrophotometer was used to assay quantitatively.

Similarly, a set of experiments by varying the adsorption time between 1 and 18 min was performed to assess the effect of increasing time on the binding capacity of MIP for adsorption kinetic experiments. In both cases, linear and nonlinear models were applied.

2.6. Imprinting Factor. The specific factor (α) for fipronil was determined by calculating the equilibrium adsorption capacities of MIP (q_m, mg g^{-1}) and NIP (q_n, mg g^{-1}) using eq 2

$$\alpha = \frac{q_m}{q_n} \tag{2}$$

2.7. Selectivity of MIPs. Cross-reactivity assays were performed to assess the ability of MIPs for the selective retention of fipronil in the presence of structurally related analogues. Fipronil was compared with chlorfenapyr, and their affinities with MIP were expressed on the basis of percentage recoveries. The DSPME conditions for these tests were the same as for the fipronil assays. The HPLC conditions reported in the literature were used for quantitative analysis.[22]

2.8. Dispersive Solid-Phase Microextraction of Fipronil from Milk Samples. The performance of the synthesized MIP was assessed by analyzing cow milk samples collected from a local area. A total of 10 mL of milk sample was taken in a centrifuge tube, and to this, $MgSO_4$ (5 g) and NaCl (1 g) were added, followed by the addition of acetonitrile (10 mL).[23] The solution was centrifuged at 8000 rpm for 10 min, and the supernatant (upper layer) was separated for further steps. The obtained upper layer was spiked at three different concentrations (0.01, 15, and 30 mg L^{-1}) of fipronil. To each concentration, 15 mg of MIP was added as the DSPME sorbent, and the mixture was shaken at optimized experimental conditions. The sample was centrifuged, and the MIP was separated from the rest of the solution. The fipronil, desorbed from the surface of the MIP using acetonitrile solvent (10 mL), was analyzed through HPLC equipped with a diode array detector (DAD). A mixture of acetonitrile/phosphate buffer (60:40, v/v) at pH 5 was used as the mobile phase. A 250 × 4.6 mm^2 long C_{18} column, whose temperature was set at 35 °C, with a diameter of 5 μm, was selected as the stationary phase. The percentage recovery of the target analyte was calculated using eq 3.

$$\text{recovery (\%)} = \frac{(C_{found} - C_{real})}{C_{real}} \times 100 \tag{3}$$

https://doi.org/10.1021/acsomega.2c05217
ACS Omega 2022, 7, 41437−41448

where C_f is the amount of fipronil determined after spiking and C_{real} and C_{added} are the actual and added amounts of the fipronil present in the sample, respectively.

3. RESULTS AND DISCUSSION

The success of the template's imprinting in a polymeric matrix mainly depends on the strong interactions between the template and the functional monomer in the prepolymerization step. In most cases, hydrogen bonding is the type of interaction that enhances the strength between the template and the monomer in the case of a noncovalent approach.[24] In this study, MIP was synthesized utilizing a simple, noncovalent method based on dipole−dipole interactions between the template and the monomer. In a prepolymerization stage, the functional groups (e.g., cyano, sulfanyl, chloro, and fluoro) possessed by the fipronil molecule facilitate hydrogen bonding with monomers, resulting in a stable template monomer complex.

The availability of many functional groups (e.g., −CO, −COOH, and −CN) on MIP that could show dipole−dipole interactions with various functional groups of fipronil was also a key factor in monomer selection. Furthermore, using three monomer MIPs (vinyl acetate, acrylic acid, and acrylonitrile) to synthesize MIP provided significant selectivity for fipronil over its structural analogues. The prepared NIP was expected to lack specific sites of recognition as it was prepared without the addition of fipronil (Figure 1).

3.1. Characterization. *3.1.1. FTIR Analysis.* FTIR analysis of both MIP and NIP (Figure 2) suggests the presence of the

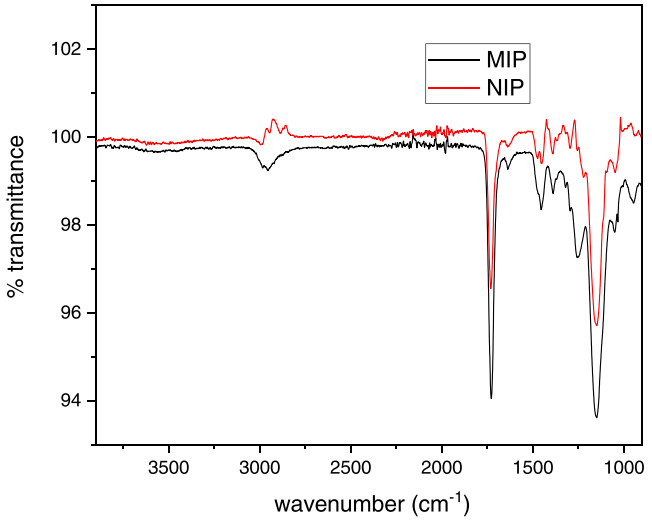

Figure 2. FTIR spectra of NIP and MIP.

C═O group as well as a less intense band of the −OH group stretching at 1727 and 3550 cm^{-1} due to carboxylic acids. The C−H stretching of methyl and unsaturated systems with sp^2 hybridization appeared at 2970 and 3070 cm^{-1}, respectively. The bands at 1450 and 1380 cm^{-1} confirm the presence of C−H bending of methylene and methyl groups. The O−H bending of carboxylic acid appeared at 1420 cm^{-1}, while the strong band at 1150 cm^{-1} is due to the C−O stretching mode.

The peak at 2241−2240 cm^{-1} could be explained by the CN of acrylonitrile. The vinyl group is attributed to the weak peaks at 910 and 994 cm^{-1}. Similarities in spectral bands confirm the presence of the same functional groups as well as the chemical composition of both MIP and NIP.

3.1.2. Thermogravimetric Analysis. The thermal stability of MIP and NIP was determined by thermogravimetric analysis (TGA). The TGA of the synthesized NIP shows a small amount of first weight loss of about 3% approximately at 60 °C, which is due to the desorption of physically absorbed water. Polymeric decomposition occurred in three prominent steps. At temperatures between 200 and 400 °C, ester bonds are expected to break, which make the major part of the polymer due to the presence of EGDMA. However, the highly crosslinked part of the NIP showed decomposition at a further elevated temperature of 500 °C. A similar trend was observed in the decomposition of MIP owing to the same precursors used for the synthesis. Thus, the similar degradation patterns confirm the same chemical structures of NIP and MIP, which further strengthens the statement that the selective adsorption of the analyte is due to the physical interaction with imprinted sites in MIP. The curves (Figure 3) show that for routine environmental sample analyses that require temperatures below 200 °C, the MIP appears quite stable and hence applicable.

3.1.3. Scanning Electron Microscopy. A clear difference in NIP and MIP particles' appearance was seen in SEM images (Figure 4). Both MIP and NIP had clustered spherical-shaped particles with a nearly uniform size and shape and appeared aggregated.

3.1.4. Nitrogen Adsorption/Desorption. Surface area and pore size of adsorbents are critical for describing adsorbent properties because they can affect analyte retention abilities. N_2 adsorption−desorption isotherm and pore size distribution for MIPs and NIPs are shown in Figure 5. MIPs showed larger pore size and pore volume than NIPs, which is possibly owing to the creation of imprinting cavities in MIPs. Using the BET technique, the specific surface area of NIP was calculated to be 58.48 $m^2\ g^{-1}$. Moreover, the mean pore volume of NIP was calculated to be 0.53 cc g^{-1}. On the other hand, MIP showed a higher surface area of 171.45 $m^2\ g^{-1}$ and a mean pore volume of 0.945 cc g^{-1}.

3.2. Cross-Reactivity. Fipronil and chlorfenapyr both have two-membered heterocyclic rings and common functional groups due to which there are maximum chances of their binding to the MIP active sites. As a result, the possibility of their affinity to MIPs cannot be ruled out, and cross-reactivity studies were done to determine their specificity. Chlorfenapyr is made up of phenyl rings with bromine, fluorine, cyano, and alkoxy groups, as shown in Figure S1. Based on structural similarities, it was predicted that the MIP would behave similarly toward both fipronil and chlorfenapyr in terms of affinity. However, the percentage recovery of chlorfenapyr was 24.8% (n = 3), while that of fipronil was found to be 94.6% (n = 3), which is a significant difference and can be attributed to the presence of specific binding sites on MIP for the fipronil structure shown in Figure 6. The MIP can thus be considered selective toward the target analyte as compared to its structural analogue.

3.3. Response Surface Methodology (RSM)−Central Composite Design (CCD). RSM not only helps in studying the interaction of independent parameters with each other and their collective effect on the dependent variable in a designed experiment but also decreases the number of experimental runs replacing the batch adsorption studies. The batch assays are mostly used for determining the optimum conditions in a

https://doi.org/10.1021/acsomega.2c05217
ACS Omega 2022, 7, 41437−41448

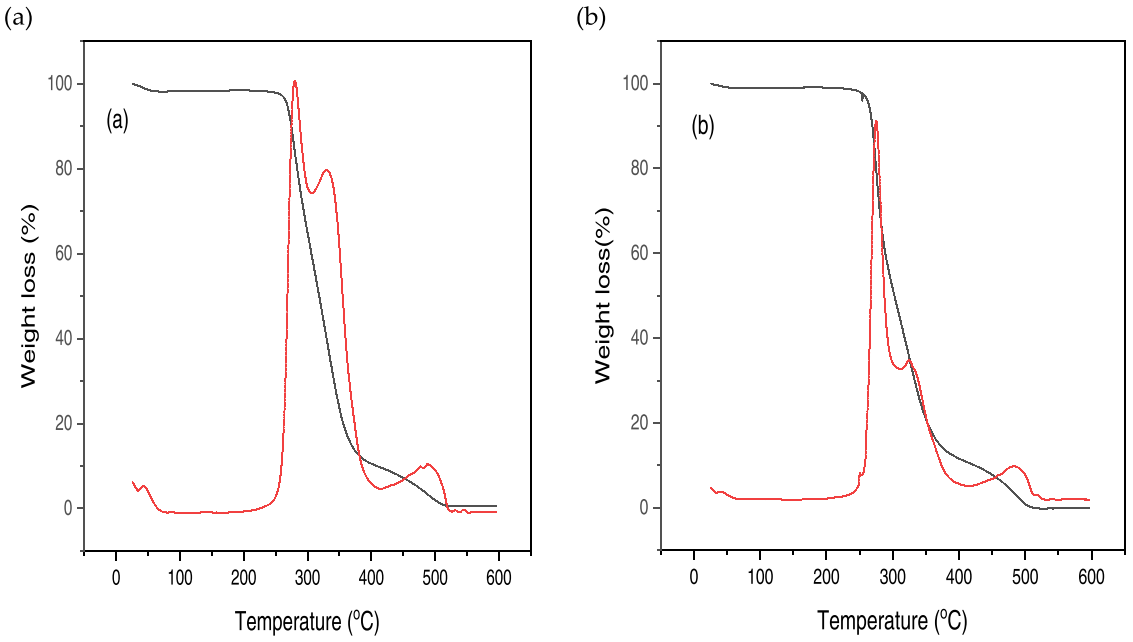

Figure 3. Study of the thermal stability of (a) NIP and (b) MIP using TGA curves.

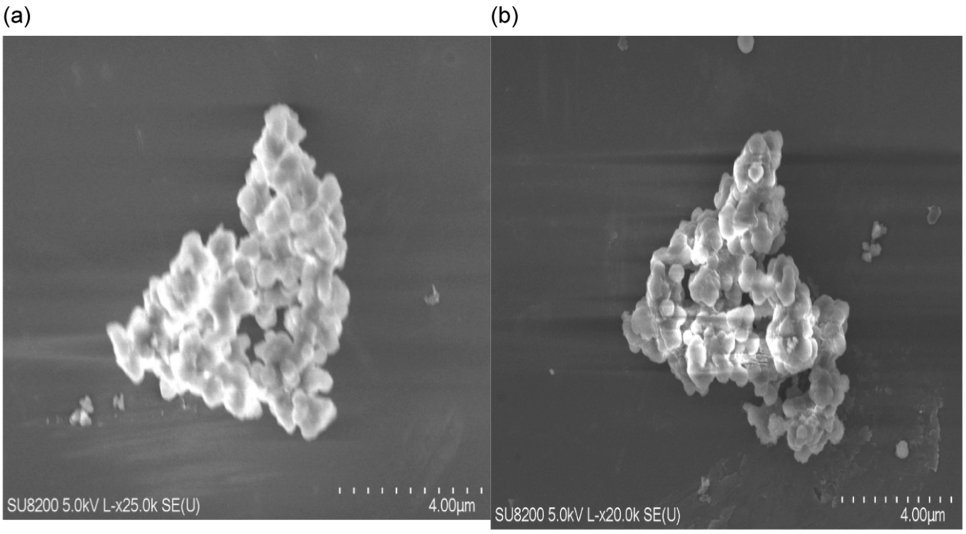

Figure 4. SEM images of (a) NIP and (b) MIP.

conventional procedure.[25] The binding capacity of MIP by changing different variables was studied by RSM. The predicted experimental sets (Table 1) for the CCD model matrix were used to calculate the binding capacity (q_e). The data followed the quadratic model (eq 4) by multiple regression analysis

$$y = \beta_0 + \sum \beta_i X_i + \sum \beta_{ij} X_i^2 + \sum \beta_{ij} X_i X_j \quad (4)$$

where β_0, β_i, β_{ii}, and β_{ij} represent intercept, linear, quadratic, and interactive model coefficients, respectively. ε and y are the random error and the predicted response, respectively. The final predicted model in terms of the coded factor is described by eq 5

$$Y = +6.06 + 0.6564A + 0.1334B + 0.0069C + 0.0238D - 0.0442AB - 0.0184AC - 0.0096AD + 0.0271BC - 0.0210BD + 0.0011CD + 0.1590A2 + 0.0686B2 - 0.0484C2 - 0.1608D2 \quad (5)$$

while eq 6 is in terms of actual parameters

https://doi.org/10.1021/acsomega.2c05217
ACS Omega 2022, 7, 41437−41448

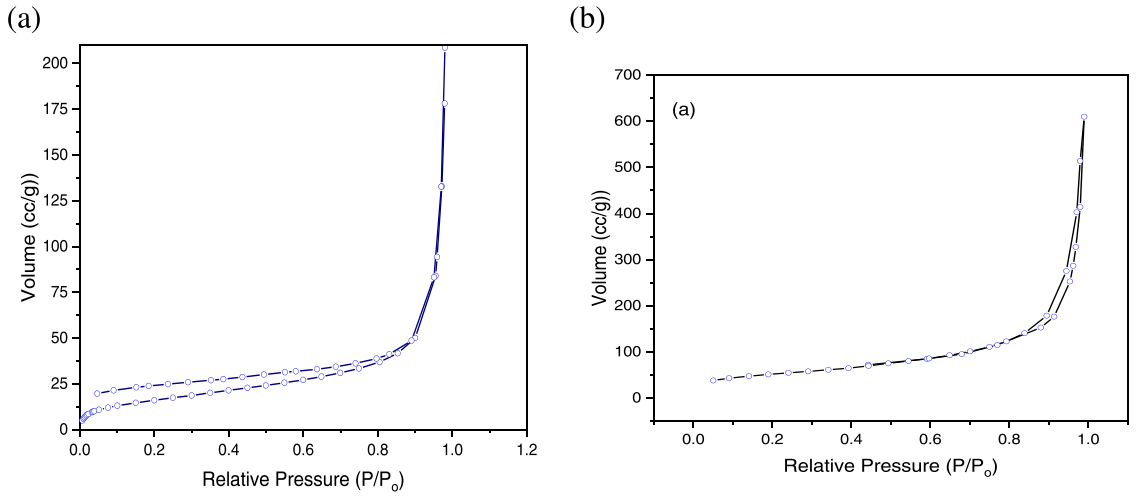

Figure 5. Nitrogen adsorption/desorption study of (a) NIP and (b) MIP.

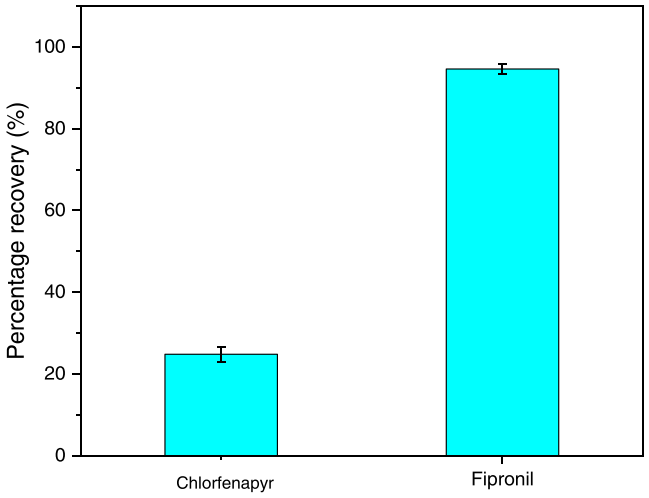

Figure 6. Percentage recovery of chlorfenapyr and fipronil on MIP.

$$Y = +\ 4.60479 + 0.006274 \times \text{concentration} + 0.000697 \times \text{pH} + 0.001872 \times \text{time}$$
$$+0.034183 \times \text{temperature} - 0.000161 \times \text{concentration} \times \text{pH} - 6.07361 \times 10^{-6} \times \text{concentration} \times \text{time}$$
$$+0.6842206 \times \text{concentration} \times \text{temperature} + 0.000098 \times \text{pH} \times \text{time} - 0.000210 \times \text{pH} \times \text{temperature}$$
$$+9.89938 \times 10^{-7} \times \text{time} \times \text{temperature} + 0.000053 \times \text{concentration}^2 + 0.002746 \times \text{pH}^2$$
$$-0.000016 \times \text{time}^2 - 0.000402 \times \text{temperature}^2 \quad (6)$$

The significance of the participant's variables in the process depends on the *P*-value. If the *P*-values are more than 0.1, then variables do not affect the process, while the essentiality of the parameters can be attributed to *P*-values less than 0.05. Fisher's *P*-value and *F*-value were 0.00001 and 147.91, respectively, which were used to confirm the applicability of the quadratic model through ANOVA statistical analysis. The lack of fit was nonsignificant with *P*-value and *F*-value of 0.7135 and 0.7041,

Table 1. Central Composite Design for Determining the Binding Capacity (q_e) of MIP

	A	B	C	D	
run	concentration (mg·L^{-1})	pH	time (min)	temperature (°C)	q_e (mg g^{-1})
1	10	12	120	60	32.0
2	65	7	65	40	37.2
3	65	7	65	40	35.5
4	10	4	10	20	27.4
5	120	4	10	60	45.0
6	10	4	120	20	27.3
7	10	12	10	20	31.2
8	10	12	10	60	29.9
9	65	7	65	20	34.6
10	120	12	120	20	46.0
11	120	4	120	20	43.9
12	65	7	10	40	35.7
13	120	7	65	40	47.0
14	65	4	65	40	35.8
15	65	7	65	40	36.5
16	120	4	10	20	44.0
17	10	7	65	40	31.6
18	10	4	120	60	28.0
19	120	4	120	60	44.1
20	65	7	65	60	35.5
21	65	12	65	40	40.0
22	10	12	120	20	32.0
23	65	7	120	40	37.1
24	120	12	10	20	46.3
25	120	12	120	60	47.0
26	10	4	10	60	28.6
27	120	12	10	60	47.0

respectively. The value of R^2 greater than 0.8 suggests that the empirical data is in agreement with the one obtained using the relevant equations.[26] The predicted and adjusted values of R^2 were 0.9708 and 0.9875, respectively, which shows reasonable agreement with each other because the difference was less than 0.2. Thus, this model can be exploited to navigate the design space.[27] The three-dimensional RSM contour plots in Figure 7 show the interaction of parameters with each other, i.e., pH, concentration, temperature, and time. The model shows that the binding capacity increases and reaches its maximum value

https://doi.org/10.1021/acsomega.2c05217
ACS Omega 2022, 7, 41437−41448

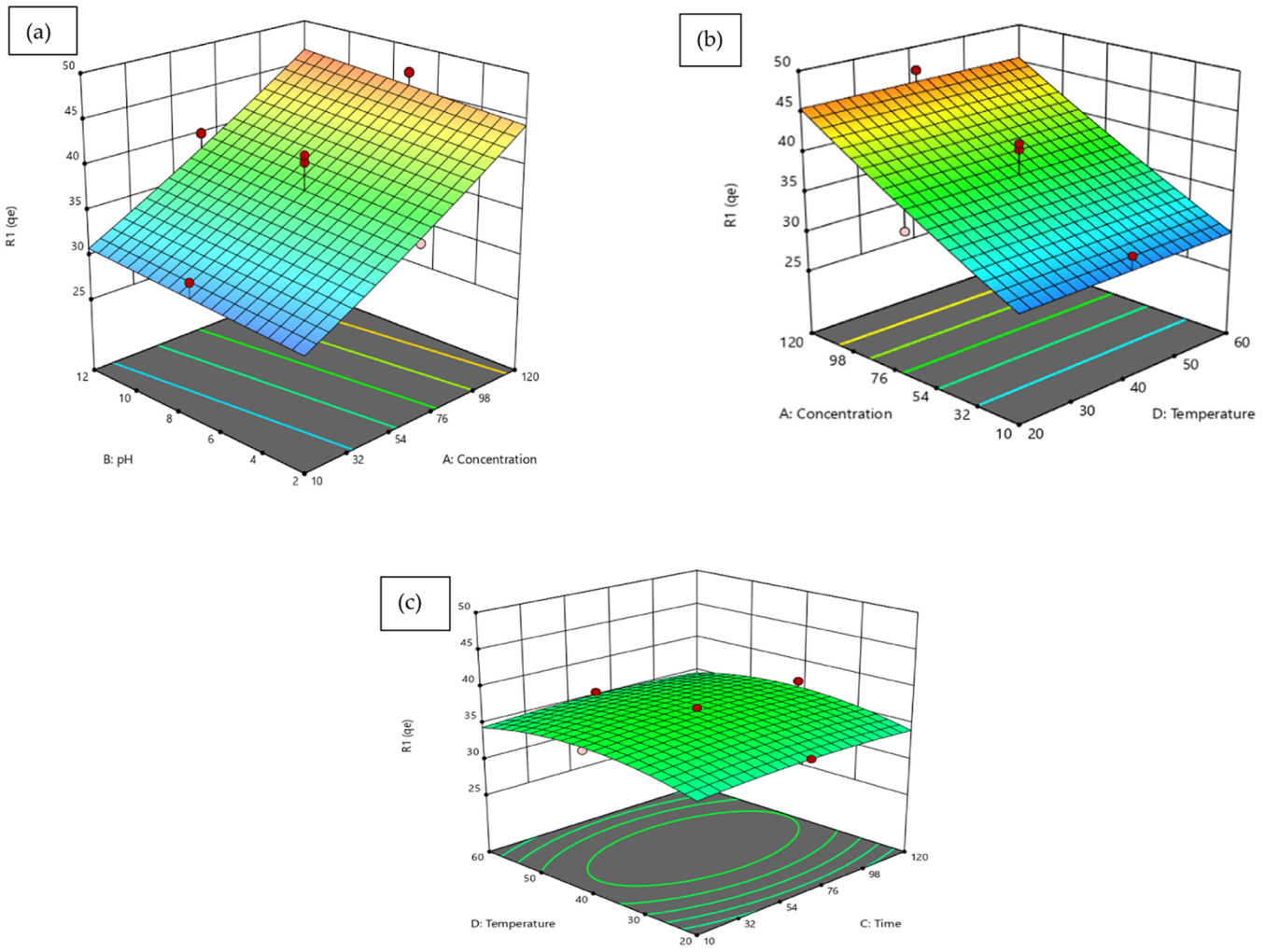

Figure 7. Interdependence of parameters and their effect on binding capacity (q_e): (a) effect of concentration and pH, (b) effect of concentration and temperature, and (c) effect of temperature and time.

at a concentration of 120 mg L^{-1}, pH 7, time 18 min, and 42 °C. Under these conditions, the model predicted a binding capacity of 47.07 mg g^{-1}. When the predicted parameters were applied experimentally, a value of 47 mg g^{-1} with a percentage error of 0.15% was obtained, which is significantly close to each other. The maximum binding at a slightly basic pH can be due to the reason that more active sites are exposed for analyte binding in a basic medium. However, there is a possibility that hydrogen ions compete with the analyte for active sites in an acidic medium. Because fipronil is less stable in alkaline conditions, there was probably less binding with a further increase in pH.[16] While evaluating the effect of temperature, it was observed that when the temperature was under 42 °C, the molecules lacked sufficient energy to penetrate the MIP and form hydrogen bonds with the inner-layer adsorption sites, resulting in inefficient adsorption mass transfer. In this situation, a higher temperature could cause an increased adsorption mass transfer of fipronil to the active sites of MIP.[28] The graph between predicted and actual values is given in Figure S2. The better distribution of the data can be explained by the points close to the straight line, which shows that actual values obeyed a specified function.

3.4. Imprint Factor. The maximum binding capacities of MIP and NIP for fipronil were determined to calculate the imprint factor. Figure 8 suggests that MIP exhibits a remarkable binding capacity relative to the NIP, which confirms the strong affinity between the imprinted site of MIP and the fipronil molecules. MIP and NIP presented

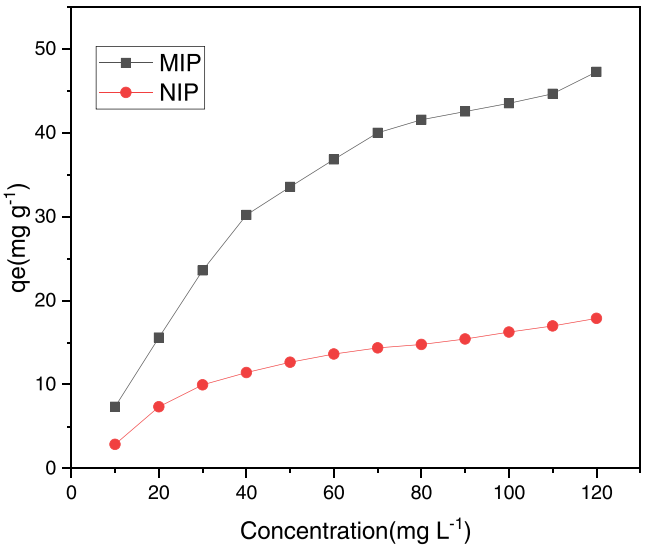

Figure 8. Comparison of the binding capacities of MIP vs NIP (n = 5).

https://doi.org/10.1021/acsomega.2c05217
ACS Omega 2022, 7, 41437−41448

maximum q_e values of 47 and 17.80 mg g^{-1}, respectively. The extent of the pesticide's adsorption on NIP can be due to the nonspecific binding sites. The relative binding capacities of both MIP and NIP can be explained by a factor known as the imprinting factor (IF). An IF value greater than 1 is acceptable for successful imprinting.[29] In this study, the IF value was 2.64, comparable to the IF of 2.02 used for the extraction of lufenuron.[20] A number of previous studies based on different templates using MIP as the sorbent have obtained comparable values. For example, the IF value for the quantification of the textile dye acid violet 19 by respective MIP in a real sample was 2.89.[30] The IF values of molecularly imprinted materials for the determination of different pesticides such as diazinon, parathion methyl, and pirimiphos-methyl were 2.88, 3.09, and 1.64, respectively.[31]

3.5. Kinetic Modeling. Kinetic-based models such as pseudo-first order and pseudo-second order have been applied to explain adsorption mechanisms and the steps for limiting adsorption rates. Various kinetic models, such as linear and nonlinear, of differing degrees of complexity are commonly used. The adsorption process is carried out by a multistep mechanism, which includes binding the analyte physically or chemically to the adsorption sites as well as mass-transfer diffusion of the analyte to the surface and into the pore. These control mechanisms are explained by the pseudo-first-order (diffusion-controlled) and pseudo-second-order (chemically controlled) kinetic models. The analyte diffusion to the adsorbent surface is the rate-determining step of the adsorption process, according to the pseudo-first-order kinetic model, while the interaction between the analyte and the adsorbent is the rate-determining step of the adsorption process, according to the pseudo-second-order kinetic model.

Nonlinear modeling has been suggested as a better method than linear regression because it provides more realistic kinetic parameters.[32] This is the first time-series modeling technique that assesses all models, allowing for a more realistic comparison to determine which model best reflects a certain kinetic data set. The discontinuity of models and the determination of any parameter before time can be minimized using this technique.[33] The best fitting of a kinetic model for adsorption studies can be explained by the low value of χ^2, the high value of R^2, and the correlation of q_e experimental values with the calculated q_e values.[34] We applied a nonlinear approach of pseudo-first-order (PFO) and pseudo-second-order (PSO) models to analyze the kinetic data. The minimum value of χ^2 (0.96) and the maximum R^2 (0.99) value close to 1 for the fipronil on the MIP indicated the best fitting of pseudo-first order (PFO). These results indicate that the fipronil molecules are adsorbed on the binding sites of MIP via a physisorption mechanism that involves a physical interaction like hydrogen bonding between the functional groups of the adsorbent and the template.[35] The nonlinear and linear forms of the PFO models are described in eqs 7 and 8, respectively. Similarly, eqs 9 and 10 relate to the nonlinear and linear PSO models, respectively.

$$q_t = q_e(1 - e^{k_1 t}) \tag{7}$$

$$\mathrm{In}(q_e - q_t) = \ln q_e - k_1 t \tag{8}$$

$$\frac{1}{q_t} = \left(\frac{1}{k2{q_e}^2}\right) \times \frac{1}{t} + \frac{1}{q_e} \tag{9}$$

$$\frac{t}{q_t} = \left(\frac{1}{k2{q_e}^2}\right) + \frac{1}{q_e} t \tag{10}$$

where q_e is the unit adsorption capacity of the MIP at adsorption equilibrium (mg g^{-1}), q_t is the unit adsorption capacity of the MIP at any time (mg g^{-1}), k_1 is the PFO rate constant (1/h), k_2 is the PSO rate constant (mg g^{-1} h^{-1}), and t is the adsorption time (h) (Figure S3).

3.6. Adsorption Isotherms. The Freundlich and Langmuir models were applied to analyze the adsorption behavior of fipronil on the corresponding MIP at an initial fipronil concentration of 15 mg L^{-1}. The linear fitting of the Freundlich and Langmuir models show R^2 values of 0.97 and 0.78, respectively. On the other hand, the nonlinear fitting models have R^2 values of 0.99 and 0.98 for Langmuir and Freundlich isotherms, respectively. Studies have shown that the determination of the best isotherm model does not depend only on the R^2 value, and to determine the best isotherm model, coupled with a higher R^2 value, there must be closeness between the data of $q_{e_{cal}}$ and $q_{e_{exp}}$.[36] In the fitted models, the q_e values are 43.25 and 60 for Freundlich and Langmuir isotherms, respectively. These results indicate the best fitting of the Freundlich isotherm, which not only has both linear and nonlinear model values close to 1 but also the q_e value is close to the calculated value. The "n" value in the Freundlich equation was close to 1, which accounts for the physical sorption of fipronil[37] (Figure S4).

The Dubinin and Radushkevich model was also applied for the adsorption study of fipronil, as shown in Figure S4c. Table S3 describes the R^2 and q_s values obtained for the model, i.e., 0.6856 and 29.785 mg g^{-1}, respectively. The mean adsorption energy (E) calculated from the Dubinin and Radushkevich model was used to ascertain the type of adsorption process under consideration.[38] If $8 > E < 16$ (lies between 8 and 16 kJ mol^{-1}), then the sorption process is chemisorption. On the other hand, if the E value is less than 8 kJ mol^{-1}, then the sorption process is physisorption.[39] The adsorption energy value, in the current work, was found to be 2.13×10^{-4} kJ mol^{-1}, which suggests the interaction to be in the range of physical adsorption reactions.[40]

3.7. Analysis of Fipronil in Milk Samples and Quality Assurance. For the selective adsorption of fipronil, the basic quality assurance (QA) parameters for the MIP-based method were evaluated in terms of precision, the limit of detection (LOD), and relative recovery. To calculate inter- and intraday precision values, three sets of experiments were performed: one each in the morning and evening, and the third one after one week, with the relative standard deviations being estimated to be 1.64% (n = 5), 1.72% (n = 5), and 1.76% (n = 5), respectively. The LOD and LOQ were calculated as 5.64×10^{-6} and 1.71×10^{-5} μg mL^{-1}, respectively. The linear range was 6×10^{-3}–45 μg mL^{-1}. The percentage recovery of fipronil was 94.6 ± 1.90% (n = 9).

Further, for real sample analysis, cow milk was collected to evaluate the effectiveness of MIP for its practical applications. The contamination of cow milk with pesticides through various pathways is becoming inevitable, and that is why a maximum residue limit of various pesticides has been established by the European Commission.[41] In analyses where a targeted detection and quantification of an analyte is required, MIP can be considered superior over other sorbents due to its specific interaction with the analyte. Thus, MIP was

https://doi.org/10.1021/acsomega.2c05217
ACS Omega 2022, 7, 41437−41448

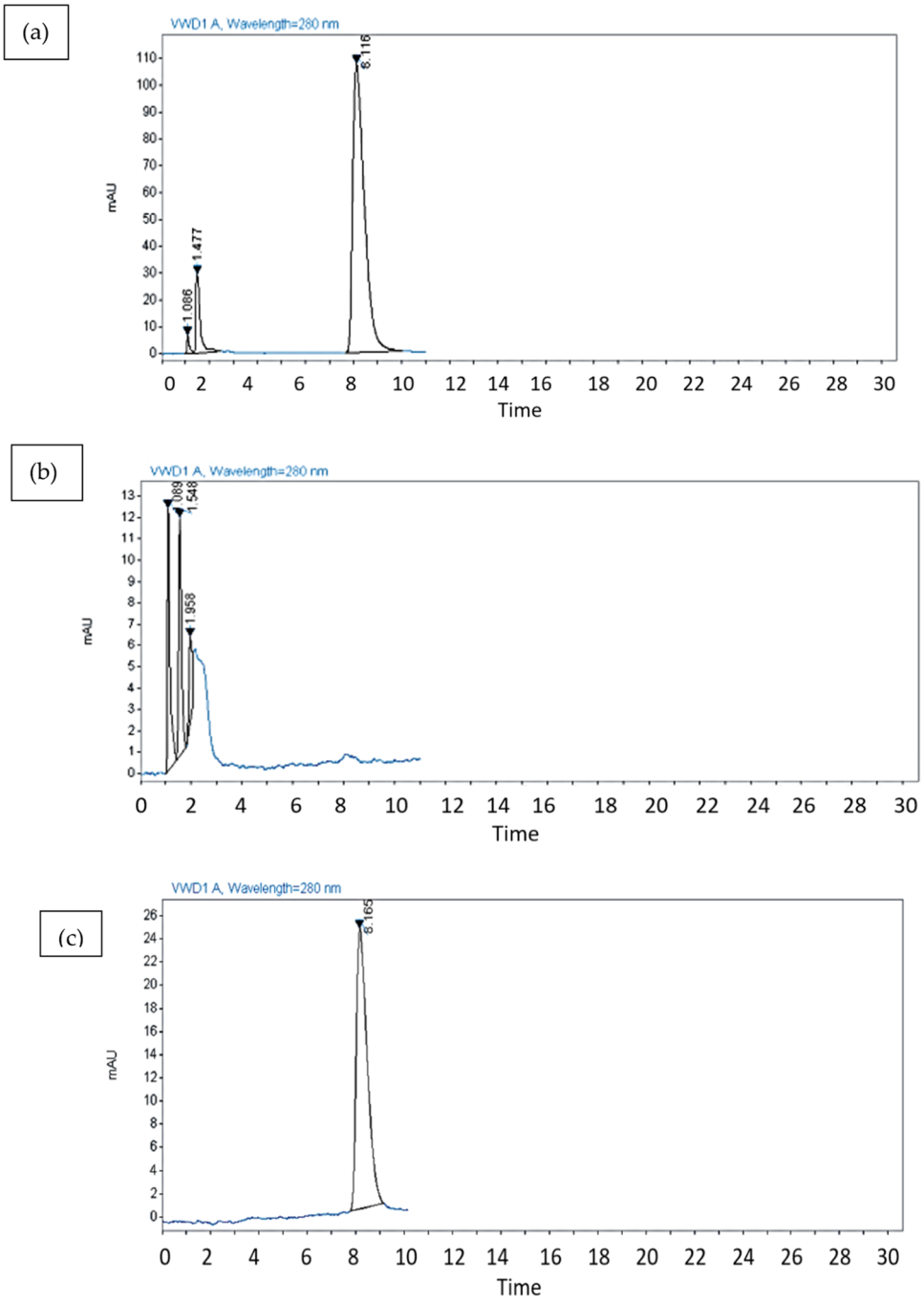

Figure 9. HPLC chromatograms of (a) the sample solution before adsorption, (b) the filtrate after the adsorption of fipronil on MIP, and (c) the desorbed fipronil that was previously loaded on MIP. HPLC conditions: C18 column, flow rate: 1.5 mL min^{-1}, and mobile phase with acetonitrile/phosphate buffer (60:40, v/v).

synthesized to be used as a DSPME sorbent for the targeted determination of fipronil from milk samples. The HPLC chromatogram of the spiked milk sample was obtained before DSPME and is shown in Figure 9a. A prominent peak of fipronil was seen at a retention time of 8.5 min. Two more peaks of unknown compounds were also observed in the sample chromatogram. Figure 9b presents the chromatogram of the solution obtained after DSPME where the fipronil peak is absent. It confirms the adsorption of fipronil on MIP during extraction. Figure 9c is the graphical display of the solution containing desorbed fipronil that was bound to MIP during the DSPME process. A single prominent peak of fipronil confirms the selectivity of MIP toward the target pesticide.

3.8. Regeneration Studies. The reusability of the MIP was tested by using it for six consecutive cycles. The first cycle's recovery rate was 94.8%; however, the subsequent cycles did not display a pronounced decrease in the percentage recovery. Furthermore, it was interesting to observe the anomaly in the sixth cycle with a slight increase in the percentage recovery. The irreversible occupancy of a small proportion of MIP's active binding sites by fipronil molecules likely caused a small decrease in recovery after six cycles (Figure S5).

https://doi.org/10.1021/acsomega.2c05217
ACS Omega 2022, 7, 41437−41448

Table 2. Comparison of the Performance of Various Adsorbents for Determining Fipronil Presence in Varied Matrixes[a]

no.	sample matrix	adsorbent	method	LOD (μg mL^{-1})	RSD	recovery, %	ref
1.	tap water	CQD@MIS	FDM	1.9×10^{-5}	1.22	91.2	42
2	oil	HA-SiO_2	SPE	3×10^{-4}–5×10^{-4}	0.9–8.7	83.0–104.0	43
3	peanut	MWCNTs	QuEChERS-LC-MS/MS	3×10^{-4}	≤19.0	66.0–116.0	44
4	maize	organic solvents	GC-ECD-SPE	5×10^{-4}–25×10^{-4}	≤8.9	83.1–106.0	45
5	milk	MIPs	DSPME	5.645×10^{-6}	1.64–1.76	94.6	current study

[a]FDM, fluorometric determination method; DSPME, dispersive solid-phase microextraction; SPE, solid-phase extraction; MIP, molecularly imprinted polymer; QuEChERS, quick, easy, cheap, effective, rugged, and safe; MWCNTs, multiwalled carbon nanotubes; HA-SiO_2, humic acid-bonded silica; CQD, carbon quantum dot; MIS, molecularly imprinted silica.

3.9. Comparative Studies. The potency of the developed method was compared with that of the already existing methods by reviewing the literature. Sorbents such as molecularly imprinted silica, carbon quantum dots (CQD@MIS),[42] and humic acid-bonded silica (HA-SiO_2)[43] were considered for comparison with newly synthesized MIPs. Moreover, the QuEChERS method using multiwalled carbon nanotubes[44] and application of organic solvents[45] has also been reported. Table 2 describes the comparison of fipronil determination using various methods. Among these studies, the current method based on the MIP sorbent had the lowest LOD and good selectivity for fipronil from milk samples.

When compared to the other insecticides of the same class, e.g., chlorfenapyr, the MIP-based sorbent showed a percentage recovery of 94.6% for fipronil in the present research. The enhanced performance of the MIP sorbent over the others for fipronil extraction can be related to the design of the imprinted cavity in the template's molecular structure.

4. CONCLUSIONS

We report here the synthesis of a molecularly imprinted polymer (MIP) as the adsorbent, its fabrication, and its application for the selective determination of fipronil in milk samples using dispersive solid-phase microextraction (DMSPE), followed by high-performance liquid chromatography (HPLC). The MIP-based method was able to determine fipronil in milk samples with a low limit of detection (5.64×10^{-65} μg mL^{-1}) and limit of quantification (1.71×10^{-5} μg mL^{-1}). This method was able to achieve a low limit of detection as compared to the published literature in this regard. The adsorptive extraction of MIPs was performed best at pH 7, with a binding capacity of 47 mg g^{-1}, which was approximately thrice that of the nonimprinted polymer (17.80 mg g^{-1}). Moreover, a high percentage recovery of 94.6% was achieved. The current study could lead to a promising strategy for extracting and analyzing trace quantities of fipronil from real samples.

■ ASSOCIATED CONTENT

Supporting Information

The Supporting Information is available free of charge at https://pubs.acs.org/doi/10.1021/acsomega.2c05217.

Structure of fipronil and chlorfenapyr; relationship between predicted and experimental values obtained through RSM; graphs of linear and nonlinear isotherms; kinetic studies; reusability of MIP; and parameters evaluated through RSM, adsorption, and kinetic models (PDF)

■ AUTHOR INFORMATION

Corresponding Authors

Suryyia Manzoor − *Institute of Chemical Sciences, Bahauddin Zakariya University, Multan 60000, Pakistan*; Email: Suryyia878@gmail.com

Noureddine Elboughdiri − *Chemical Engineering Department, College of Engineering, University of Ha'il, Ha'il 81441, Saudi Arabia; Chemical Engineering Process Department, National School of Engineers Gabes, University of Gabes, Gabes 6029, Tunisia*; orcid.org/0000-0003-2923-3062; Email: ghilaninouri@yahoo.fr

Authors

Muhammad Hayat − *Institute of Chemical Sciences, Bahauddin Zakariya University, Multan 60000, Pakistan*

Nadeem Raza − *Department of Chemistry, Emerson University, Multan 60000, Pakistan*

Akmal Abbas − *State Key Laboratory of Fine Chemicals, PSU-DUT Joint Center of Energy and Research, School of Chemical Engineering, Dalian University of Technology, Dalian 116024, China*

Muhammad Imran Khan − *Research Institute of Sciences and Engineering (RISE), University of Sharjah, Sharjah 27272, United Arab Emirates*

Khalida Naseem − *Department of Basic and Applied Chemistry, Faculty of Science and Technology, University of Central Punjab, Lahore 54700, Pakistan*

Abdallah Shanableh − *Research Institute of Sciences and Engineering (RISE), University of Sharjah, Sharjah 27272, United Arab Emirates*

Abdullah M. M. Elbadry − *Faculty of Pharmacy, Badr University in Cairo (BUC), Cairo 11829, Egypt*; orcid.org/0000-0003-4495-1556

Saleh Al Arni − *Chemical Engineering Department, College of Engineering, University of Ha'il, Ha'il 81441, Saudi Arabia*

Mhamed Benaissa − *Chemical Engineering Department, College of Engineering, University of Ha'il, Ha'il 81441, Saudi Arabia*; orcid.org/0000-0002-5639-6169

Fatma A. Ibrahim − *Catalysis Research Group (CRG), Department of Chemistry, Faculty of Science, King Khalid University, Abha 61413, Saudi Arabia*

Complete contact information is available at: https://pubs.acs.org/10.1021/acsomega.2c05217

Notes

The authors declare no competing financial interest.

■ ACKNOWLEDGMENTS

This research was funded by the Research Deanship of University of Ha'il, Saudi Arabia, through Project RG-21 036. The authors are grateful to Bahauddin Zakariya University,

Multan, Pakistan, and Dalian University of Technology, Dalian, China, for providing the lab facility to conduct this research work.

REFERENCES

(1) Donley, N. The USA lags behind other agricultural nations in banning harmful pesticides. *Environ. Health* **2019**, *18*, 44.
(2) Silva, M. P.; Tubino, M.; Elsholz, T. C.; Elsholz, O.; Khan, S.; Vila, M. M. Flow injection analysis system for screening organophosphorus pesticides by their inhibitory effect on the enzyme acethylcholinesterase. *J. Braz. Chem. Soc.* **2015**, *26*, 484−489.
(3) Silva, V.; Mol, H. G.; Zomer, P.; Tienstra, M.; Ritsema, C. J.; Geissen, V. Pesticide residues in European agricultural soils−A hidden reality unfolded. *Sci. Total Environ.* **2019**, *653*, 1532−1545.
(4) Lehmann, E.; Fargues, M.; Nfon Dibié, J.-J.; Konaté, Y.; de Alencastro, L. F. Assessment of water resource contamination by pesticides in vegetable-producing areas in Burkina Faso. *Environ. Sci. Pollut. Res.* **2018**, *25*, 3681−3694.
(5) Abou-Arab, A.; Abou Donia, M. Pesticide residues in some Egyptian spices and medicinal plants as affected by processing. *Food Chem.* **2001**, *72*, 439−445.
(6) Gunasekara, A. S.; Truong, T.; Goh, K. S.; Spurlock, F.; Tjeerdema, R. S. Environmental fate and toxicology of fipronil. *J. Pestic. Sci.* **2007**, *32*, 189−199.
(7) Simon-Delso, N.; Amaral-Rogers, V.; Belzunces, L. P.; Bonmatin, J.-M.; Chagnon, M.; Downs, C.; Furlan, L.; Gibbons, D. W.; Giorio, C.; Girolami, V.; et al. Systemic insecticides (neonicotinoids and fipronil): trends, uses, mode of action and metabolites. *Environ. Sci. Pollut. Res.* **2015**, *22*, 5−34.
(8) Wang, X.; Martínez, M. A.; Wu, Q.; Ares, I.; Martínez-Larrañaga, M. R.; Anadón, A.; Yuan, Z. Fipronil insecticide toxicology: oxidative stress and metabolism. *Crit. Rev. Toxicol.* **2016**, *46*, 876−899.
(9) Van der Sluijs, J. P.; Amaral-Rogers, V.; Belzunces, L. P.; Bijleveld van Lexmond, M. F.; Bonmatin, J.-M.; Chagnon, M.; Downs, C.; Furlan, L.; Gibbons, D. W.; Giorio, C.; et al. Conclusions of the Worldwide Integrated Assessment on the risks of neonicotinoids and fipronil to biodiversity and ecosystem functioning. *Environ. Sci. Pollut. Res.* **2015**, *22*, 148−154.
(10) Pisa, L.; Goulson, D.; Yang, E.-C.; Gibbons, D.; Sánchez-Bayo, F.; Mitchell, E.; Aebi, A.; van der Sluijs, J.; MacQuarrie, C. J.; Giorio, C.; et al. An update of the Worldwide Integrated Assessment (WIA) on systemic insecticides. Part 2: impacts on organisms and ecosystems. *Environ. Sci. Pollut. Res.* **2021**, *28*, 11749−11797.
(11) Pisa, L. W.; Amaral-Rogers, V.; Belzunces, L. P.; Bonmatin, J.-M.; Downs, C. A.; Goulson, D.; Kreutzweiser, D. P.; Krupke, C.; Liess, M.; McField, M.; et al. Effects of neonicotinoids and fipronil on non-target invertebrates. *Environ. Sci. Pollut. Res.* **2015**, *22*, 68−102.
(12) Mandal, K.; Singh, B.; Jariyal, M.; Gupta, V. Bioremediation of fipronil by a Bacillus firmus isolate from soil. *Chemosphere* **2014**, *101*, 55−60.
(13) Romeh, A. A. A. Green silver nanoparticles for enhancing the phytoremediation of soil and water contaminated by fipronil and degradation products. *Water, Air, Soil Pollut.* **2018**, *229*, 147.
(14) Bonmatin, J.-M.; Giorio, C.; Girolami, V.; Goulson, D.; Kreutzweiser, D.; Krupke, C.; Liess, M.; Long, E.; Marzaro, M.; Mitchell, E. A.; et al. Environmental fate and exposure; neonicotinoids and fipronil. *Environ. Sci. Pollut. Res.* **2015**, *22*, 35−67.
(15) Le Faouder, J.; Bichon, E.; Brunschwig, P.; Landelle, R.; Andre, F.; Le Bizec, B. Transfer assessment of fipronil residues from feed to cow milk. *Talanta* **2007**, *73*, 710−717.
(16) Singh, N. S.; Sharma, R.; Singh, S. K.; Singh, D. K. A comprehensive review of environmental fate and degradation of fipronil and its toxic metabolites. *Environ. Res.* **2021**, *199*, No. 111316.
(17) Hassaan, M. A.; El Nemr, A. Pesticides pollution: Classifications, human health impact, extraction and treatment techniques. *Egypt. J. Aquat. Res.* **2020**, *46*, 207−220.
(18) Pan, C.; Wang, L.Application of DART-MS in Foods and Agro-Products Analysis. In *Direct Analysis in Real Time Mass Spectrometry: Principles and Practices of DART-MS*; Wiley, 2018; pp 133−161.
(19) Guć, M.; Messyasz, B.; Schroeder, G. Environmental impact of molecularly imprinted polymers used as analyte sorbents in mass spectrometry. *Sci. Total Environ.* **2021**, *772*, No. 145074.
(20) Hayat, M.; Raza, N.; Jamal, U.; Manzoor, S.; Abbas, N.; Khan, M. I.; Lee, J.; Brown, R. J.; Kim, K.-H. Targeted extraction of pesticide from agricultural run-off using novel molecularly imprinted polymeric pendants. *J. Ind. Eng. Chem.* **2022**, *109*, 202−209.
(21) Khezeli, T.; Daneshfar, A. Development of dispersive micro-solid phase extraction based on micro and nano sorbents. *TrAC, Trends Anal. Chem.* **2017**, *89*, 99−118.
(22) Hafeez, A.; Tawab, I. A.; Iqbal, S. Development and validation of an HPLC method for the simultaneous determination of fipronil, chlorfenapyr, and pyriproxyfen in insecticide formulations. *J. AOAC Int.* **2016**, *99*, 1185−1190.
(23) Jawaid, S.; Talpur, F. N.; Nizamani, S. M.; Khaskheli, A. A.; Afridi, H. Multipesticide residue levels in UHT and raw milk samples by GC-μECD after QuEChER extraction method. *Environ. Monit. Assess.* **2016**, *188*, 230.
(24) Fu, X.; Yang, Q.; Zhou, Q.; Lin, Q.; Wang, C. Template-monomer interaction in molecular imprinting: is the strongest the best? *Open J. Org. Polym. Mater.* **2015**, *05*, 58.
(25) Wei, Y.; Khoza, T.; Yu, Y.; Wang, L.; Liu, B.; Wang, J.; Gan, L.; Hao, F.; Shao, G.; Feng, Z.; Xiong, Q. Development of an indirect competitive enzyme linked immunosorbent assay for the quantitative detection of Mycoplasma hyopneumoniae during the vaccine production process. *J. Immunol. Methods* **2022**, *500*, No. 113196.
(26) Dashti, A. F.; Adlan, M. N.; Abdul Aziz, H.; Ibrahim, A. H. Application of response surface methodology (RSM) for optimization of ammoniacal nitrogen removal from palm oil mill wastewater using limestone roughing filter. *J. Appl. Res. Water Wastewater* **2018**, *5*, 411−416.
(27) Arslan-Alaton, I.; Tureli, G.; Olmez-Hanci, T. Treatment of azo dye production wastewaters using Photo-Fenton-like advanced oxidation processes: Optimization by response surface methodology. *J. Photochem. Photobiol. A* **2009**, *202*, 142−153.
(28) Feng, C.; Jiaqiang, E.; Han, W.; Deng, Y.; Zhang, B.; Zhao, X.; Han, D. Key technology and application analysis of zeolite adsorption for energy storage and heat-mass transfer process: A review. *Renewable Sustainable Energy Rev.* **2021**, *144*, No. 110954.
(29) Ndunda, E. N. Molecularly imprinted polymers-A closer look at the control polymer used in determining the imprinting effect: A mini review. *J. Mol. Recognit.* **2020**, *33*, No. e2855.
(30) Quinto, M. L.; Khan, S.; Picasso, G.; Sotomayor, M. D. P. T. Synthesis, characterization, and evaluation of a selective molecularly imprinted polymer for quantification of the textile dye acid violet 19 in real water samples. *J. Hazard. Mater.* **2020**, *384*, No. 121374.
(31) Xiang, X.; Wang, Y.; Zhang, X.; Huang, M.; Li, X.; Pan, S. Multifiber solid-phase microextraction using different molecularly imprinted coatings for simultaneous selective extraction and sensitive determination of organophosphorus pesticides. *J. Sep. Sci.* **2020**, *43*, 756−765.
(32) Karadag, D.; Koc, Y.; Turan, M.; Ozturk, M. A comparative study of linear and non-linear regression analysis for ammonium exchange by clinoptilolite zeolite. *J. Hazard. Mater.* **2007**, *144*, 432−437.
(33) Franceschini, G.; Macchietto, S. Model-based design of experiments for parameter precision: State of the art. *Chem. Eng. Sci.* **2008**, *63*, 4846−4872.
(34) Sahoo, T.; Prelot, B.Nanomaterials for the Detection and Removal of Wastewater Pollutants. In *Adsorption Processes for the Removal of Contaminants from Wastewater: The Perspective Role of Nanomaterials and Nanotechnology*; Elsevier, 2020; Chapter 7, pp 161−222.
(35) De Oliveira, H. L.; Pires, B. C.; Teixeira, L. S.; Dinali, L. A. F.; do Nascimento, T. A.; Borges, K. B. Mesoporous molecularly

https://doi.org/10.1021/acsomega.2c05217
ACS Omega 2022, 7, 41437−41448

imprinted polymer for removal of hormones from aqueous medium. *Colloids Surf., A* **2020**, *590*, No. 124506.
(36) Ojediran, J. O.; Dada, A. O.; Aniyi, S. O.; David, R. O.; Adewumi, A. D. Mechanism and isotherm modeling of effective adsorption of malachite green as endocrine disruptive dye using Acid Functionalized Maize Cob (AFMC). *Sci. Rep.* **2021**, *11*, No. 21498.
(37) Bobé, A.; Coste, C. M.; Cooper, J.-F. Factors influencing the adsorption of fipronil on soils. *J. Agric. Food Chem.* **1997**, *45*, 4861−4865.
(38) Walton, H.*Ion Exchange in Analytical Chemistry*; ACS Publications, 1965.
(39) Bezzina, J. P.; Robshaw, T.; Dawson, R.; Ogden, M. D. Single metal isotherm study of the ion exchange removal of Cu (II), Fe (II), Pb (II) and Zn (II) from synthetic acetic acid leachate. *Chem. Eng. J.* **2020**, *394*, No. 124862.
(40) Khan, A. A.; Singh, R. Adsorption thermodynamics of carbofuran on Sn (IV) arsenosilicate in H+, Na+ and Ca2+ forms. *Colloids Surf.* **1987**, *24*, 33−42.
(41) Wu, X.; Tong, K.; Yu, C.; Hou, S.; Xie, Y.; Fan, C.; Chen, H.; Lu, M.; Wang, W. Development of a High-Throughput Screening Analysis for 195 Pesticides in Raw Milk by Modified QuEChERS Sample Preparation and Liquid Chromatography Quadrupole Time-of-Flight Mass Spectrometry. *Separations* **2022**, *9*, 98.
(42) Yang, C.; Wang, L.; Zhang, Z.; Chen, Y.; Deng, Q.; Wang, S. Fluorometric determination of fipronil by integrating the advantages of molecularly imprinted silica and carbon quantum dots. *Microchim. Acta* **2020**, *187*, 12.
(43) Peng, X. T.; Li, Y. N.; Xia, H.; Peng, L. J.; Feng, Y. Q. Rapid and sensitive detection of fipronil and its metabolites in edible oils by solid-phase extraction based on humic acid bonded silica combined with gas chromatography with electron capture detection. *J. Sep. Sci.* **2016**, *39*, 2196−2203.
(44) Li, M.; Li, P.; Wang, L.; Feng, M.; Han, L. Determination and dissipation of fipronil and its metabolites in peanut and soil. *J. Agric. Food Chem.* **2015**, *63*, 4435−4443.
(45) Wang, T.; Hu, J.; Liu, C. Simultaneous determination of insecticide fipronil and its metabolites in maize and soil by gas chromatography with electron capture detection. *Environ. Monit. Assess.* **2014**, *186*, 2767−2774.

https://doi.org/10.1021/acsomega.2c05217
ACS Omega 2022, 7, 41437−41448